

INTERACTION OF 80 to 300 Mev  $\pi^+$  MESONS WITH LIGHT NUCLEI

G. A. BLINOV, M. F. LOMANOV, Ia. Ia. SHALAMOV, V. A. SHEBANOV, and V. A. SHCHEGOLEV

Submitted to JETP editor May 6, 1958

J. Exptl. Theoret. Phys. (U.S.S.R.) **35**, 880-886 (October, 1958)

A 17-liter bubble chamber was used to study the interaction of  $\pi^+$  mesons with nuclei. The cross-sections for scattering, absorption, charge-exchange scattering, and production of charged mesons were measured. The processes of absorption and charge-exchange scattering are discussed.

A bubble chamber filled with a mixture of freons  $\text{CCl}_2\text{F}_2$  and  $\text{CClF}_3$  was used for experiments on the interaction of 80 to 300 Mev  $\pi^+$  mesons with the working liquid in the chamber. The cross sections for charge-exchange scattering and star production, and the total cross section for elastic and inelastic scattering in collisions between  $\pi^+$  mesons and C, F, and Cl nuclei were measured for ten energy values throughout the range. Six events in which charged  $\pi$  mesons had been produced by  $\pi^+$  mesons were observed in the 210 to 300 Mev range. The cross section for charge-exchange scattering was found to increase by a factor of two over the 80 to 200 Mev range, attaining 10% of the geometrical cross section. The star-production cross section reaches a maximum in the vicinity of 180 Mev. Experiments were carried out on the interaction of 260 Mev protons stopping in the chamber.

A comparison of the stars accompanying the charge-exchange scattering events with those produced in interactions of protons with C, F, and Cl nuclei shows that the charge-exchange scattering on light nuclei is a result of the interaction between the incident  $\pi^+$  meson and a single nucleon of the nucleus. An analysis of the absorption stars and comparison with proton-produced stars shows that, in the energy range investigated, the absorption of  $\pi^+$  mesons results predominantly from a single interaction between the  $\pi^+$  meson and a proton-neutron pair. This process occurs in 60 to 70% of the events involving 200-Mev  $\pi^+$  mesons.

## 1. EXPERIMENTAL METHOD

The experiments were made with the synchrocyclotron of the Nuclear Research Laboratory of the Joint Institute for Nuclear Research. The  $\pi^+$ -meson beams were obtained by bombarding polyethylene targets with the external proton beam.<sup>1</sup> A  $\pi^+$  meson beam of given energy traversed the freon bubble chamber having an observation vol-

ume of  $50 \times 22 \times 15 \text{ cm}^3$ . The construction and operation of the chamber have been described in an earlier publication.<sup>2</sup> The working liquid used in this series of experiments consisted of a mixture of 54% (per weight) freon 12 ( $\text{CCl}_2\text{F}_2$ ) and 46% freon 13 ( $\text{CClF}_3$ ). The chamber operated at  $+28^\circ\text{C}$ . The working liquid density was equal to  $1.12 \text{ g/cm}^3$ . When the chamber was triggered, its pressure fell from 38 to 10 or 13 atmos in about 15 milliseconds. The fact that the pressure dropped to a predetermined level ensured a good stability of the chamber sensitivity, and made it possible to choose quickly the working conditions during the experiments. The operating cycle of the chamber varied from 16 to 40 sec in different experiments. A stereoscopic camera using two parallel films, with a lens base of 103 mm and mean reduction equal to 11.6 was used for photography.

Since the  $\pi^+$  mesons lost by ionization about 80 Mev in traversing the chamber, it was possible to study the interaction of  $\pi^+$  mesons of various energies using a single beam. The chamber volume was divided for that purpose into four regions by means of a grid on the internal side of plexiglass windows. The grid simplified also considerably coordinate measurements in the chamber.

Three series of measurements were conducted, with the initial energy of  $\pi^+$  mesons in the beam (before entering the chamber) equal to 320, 234, and 130 Mev respectively. The 320 Mev and 230 Mev beams were obtained choosing the field of the deflecting magnet so that the maximum beam intensity was attained for a given thickness of the polyethylene target bombarded by protons. The secondary  $\pi^+$  meson beam was produced mainly as the result of the  $pp \rightarrow d\pi^+$  reaction. It was difficult to find experimentally the maximum intensity of the 130 Mev beam and the corresponding setting of the magnetic field was calculated.

The energy of  $\pi^+$  mesons in the first beam

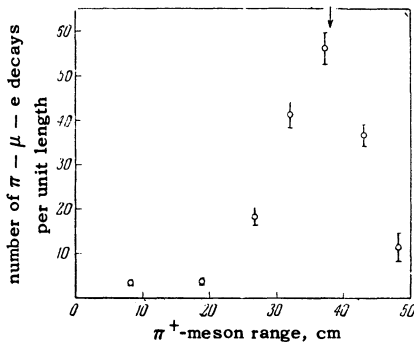


FIG. 1. Dependence of the number of  $\pi-\mu-e$  decays per unit length on the  $\pi^+$ -meson range.

(320 Mev) was found from the kinetics of the reaction  $pp \rightarrow d\pi^+$  taking into account the ionization losses in the polyethylene target and in the layer of air between the target and the chamber. The energy of  $\pi^+$  mesons in the other beams was obtained from the energy of the first beam and the relative magnetic field intensities. The energy of the third beam calculated in that way (130 Mev) is in a good agreement with that found from the range-energy relation  $R(E)$ . The range of  $\pi^+$  mesons in the chamber was measured by counting the number of  $\pi-\mu-e$  decays along the  $\pi^+$ -meson path. The results are shown in Fig. 1, where the arrow indicates the  $\pi^+$ -meson range calculated from the range-energy curves under the assumption that the energy of the  $\pi^+$  mesons was 130 Mev before entering the chamber.

Possible admixture of other particles in the  $\pi^+$ -meson beam was taken into account in counting the number of  $\pi^+$  mesons traversing the chamber. Proton and electron tracks were easily distinguished by their ionization and multiple scattering, so that their presence did not introduce any errors. The admixture of  $\mu$  mesons in the 130-Mev beam amounted to 13%. This value was found from the pictures by means of data on the range of  $\pi$  and  $\mu$  mesons. We did not determine the fraction of  $\mu$  mesons in the other beams, but used the results of Mukhin et al.<sup>1</sup> who conducted experiments in identical conditions. Data on the admixture of  $\mu$  mesons were taken into account in calculating the cross sections. In addition, a correction was applied for the  $\pi^+$  mesons removed from the beam by multiple scattering.

Only  $\pi^+$  mesons entering the chamber at not more than  $5^\circ$  to the beam axis and not less than 7 cm from the top and bottom wall of the chamber were counted. The  $\pi^+$  mesons that underwent an interaction were identified by their ionization, multiple scattering, or  $\pi-\mu-e$  decay. In several cases  $\pi^+$  mesons were identified by the characteristic increase of ionization and multiple scat-

TABLE I. Cross-sections for various interactions of  $\pi^+$  mesons with C, F, and Cl nuclei expressed in terms of the mean geometrical cross-section

$\pi^+$ meson energy, Mev	$\sigma_e/\sigma_{geom}^*$	$\sigma_a/\sigma_{geom}$	$\sigma_s/\sigma_{geom}$
77	$0.045 \pm 0.020$	$0.393 \pm 0.050$	$0.491 \pm 0.056$
100	$0.068 \pm 0.023$	$0.502 \pm 0.055$	$0.807 \pm 0.068$
136	$0.064 \pm 0.025$	$0.537 \pm 0.064$	$0.904 \pm 0.084$
157	$0.101 \pm 0.028$	$0.629 \pm 0.068$	$1.056 \pm 0.089$
177	$0.092 \pm 0.023$	$0.572 \pm 0.058$	$1.108 \pm 0.083$
197	$0.078 \pm 0.019$	$0.549 \pm 0.051$	$1.144 \pm 0.081$
224	$0.107 \pm 0.022$	$0.447 \pm 0.059$	$0.973 \pm 0.092$
245	$0.099 \pm 0.020$	$0.439 \pm 0.053$	$1.050 \pm 0.087$
264	$0.124 \pm 0.020$	$0.365 \pm 0.041$	$1.032 \pm 0.079$
283	$0.098 \pm 0.016$	$0.375 \pm 0.042$	$0.886 \pm 0.067$

\*Only statistical errors are given.

tering along the track. Only the events in which the sum of the scattering angle projections in the two pictures was larger than  $10^\circ$  were used for measuring the scattering cross-section. The adoption of this criterion prevented the errors due to the multiple scattering and decay of  $\pi$  mesons in flight.

The large dimensions of the bubble chamber and the relatively high density of the filling liquid ensured a high efficiency of photon detection through pair production. It was therefore possible to measure separately the cross sections for star production and charge-exchange scattering ( $\pi^+ \rightarrow \pi^0$ ). In the reduction of the data, events in which the disappearance of a  $\pi^+$  meson was accompanied by one or two conversion pairs with their apex directed towards the point in which the interaction took place were interpreted as charge-exchange scattering. The accuracy with which the pair followed the direction of the photon amounted to  $\pm 3$  or  $5^\circ$  and was determined from the mean angle of multiple scattering of the electrons and

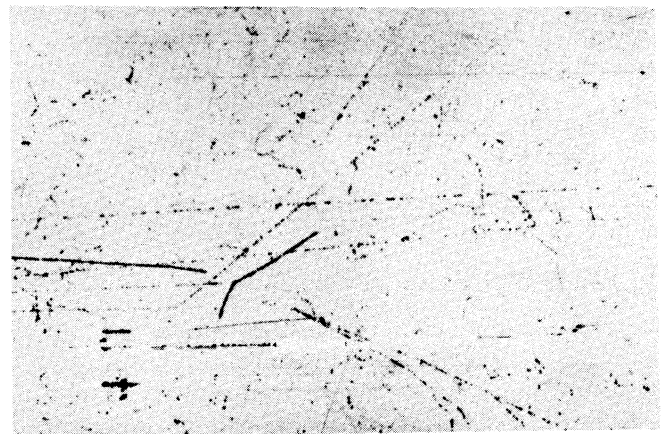


FIG. 2. Photograph of a charge-exchange scattering event. The conversion pair is produced by a photon emitted from the two-pronged star.



FIG. 3. A charge-exchange scattering event. Two conversion pairs are visible.

the mean angle between the momentum of the photon and of the pair.

The efficiency of  $\pi^0$ -meson detection in the chamber was calculated by two methods. In the first, the probability of the materialization of photons within a sphere 5 cm in radius was calculated using the known value of the radiation length, equal to 21.2 cm for the case of the freon mixture used, under the condition that the angle between the direction of emission of photons and the film plane was  $\leq 30^\circ$ . The calculation showed that the probability that a conversion pair will be observed in this volume is 0.21. The detection efficiency for charge-exchange scattering events is then  $0.21 N_0/N_1$ , where  $N_0$  is the total number of pairs produced in the total volume of the chamber, and  $N_1$  is the number of pairs found within a sphere 5 cm in radius.

In the second method we studied the characteristic features of the stars accompanying charge-exchange scattering events. It was found that in the majority of cases the energy of protons in

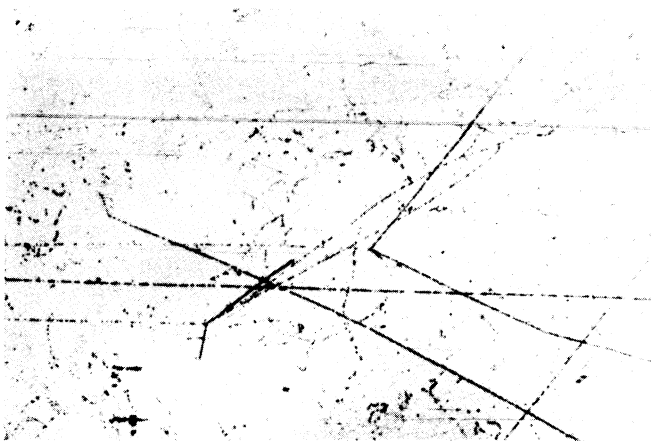


FIG. 4. A charge-exchange scattering event. A  $\pi^0$ -meson decays according to the scheme  $\pi^0 \rightarrow e^+ + e^- + \gamma$ .

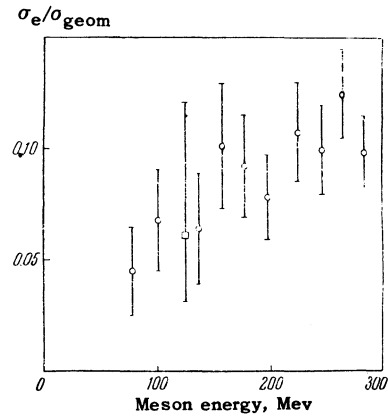


FIG. 5. Energy dependence of the charge-exchange scattering cross sections of  $\pi^+$  mesons. O — this experiment,  $\square$  — ( $\pi^+$ , C) according to reference 10.

these was less than 30 or 40 Mev. The multiplicity distribution of stars unaccompanied by a conversion pair is similar to that of stars associated with exchange scattering. One can assume, therefore, that all stars with a low energy yield correspond to exchange scattering events, i.e., that the detection probability of  $\pi^0$  mesons is given by the ratio of the number of stars accompanied by a conversion pair to the total number of low-energy stars. Both methods yielded similar results for the  $\pi^0$ -meson detection efficiency, which was found to be equal to  $0.50 \pm 0.11$ .

## 2. RESULTS AND DISCUSSION

About 7000 pairs of photographs were taken while the chamber was exposed to the  $\pi^+$  beams. 193 exchange-scattering events and six charged-meson production events were detected in the energy range from 80 to 300 Mev. In the scanning of 3000 pictures, 4460 various interaction events of  $\pi^+$  mesons with nuclei were observed. Examples of the pictures are shown in Figs. 2 to 4.

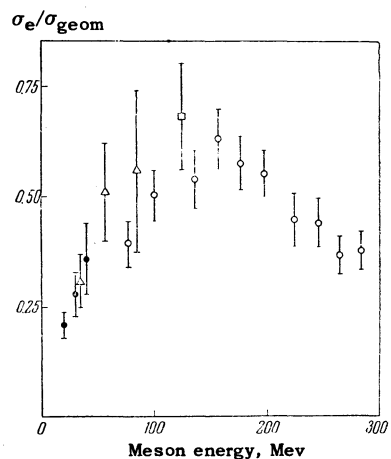


FIG. 6. Energy dependence of the star-production cross sections of  $\pi^+$  mesons. O — this experiment,  $\square$  — ( $\pi^+$ , C),<sup>10</sup>  $\Delta$  — ( $\pi^+$  Al),<sup>5</sup>  $\bullet$  — ( $\pi^+$ , Be).<sup>7</sup>

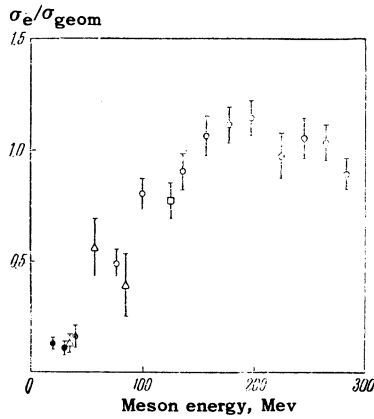


FIG. 7. Energy dependence of the total cross section for elastic and inelastic scattering of  $\pi^+$  mesons.  $\circ$  - this experiment,  $\square$  - ( $\pi^+$ , C),<sup>10</sup>  $\triangle$  - ( $\pi^+$ , Al),<sup>5</sup>  $\bullet$  - ( $\pi^+$ , Be).<sup>7</sup>

The observed energy dependence of the various types of interaction of  $\pi^+$  mesons is given in Table I. In this table  $\sigma_e$  denotes the exchange scattering cross section,  $\sigma_a$  is the star production (absorption) cross-section, and  $\sigma_s$  is the total cross section for elastic and inelastic scattering. The measured value of the latter was somewhat low, since we considered only those scattering events in which the sum of the scattering angle projections in both pictures was larger than  $10^\circ$ . All cross sections in the table are expressed in terms of the mean geometrical cross-section of the C, F, and Cl nuclei, equal to  $483 \times 10^{-27} \text{ cm}^2$ . This value was calculated assuming a nuclear radius of  $1.40 \times 10^{-13} A^{1/3}$ . The energy dependence of the cross-sections  $\sigma_e$ ,  $\sigma_a$ ,  $\sigma_s$ , constructed using the data of Table I, is shown in Figs. 5 to 7.

The multiplicity distribution of stars was studied in order to elucidate the mechanism of the charge-exchange scattering of  $\pi^+$  mesons and their absorption by nuclei. Charged star products were recorded starting with 10 to 20 Mev proton energy. Most detailed data on the multiplicity distribution were obtained for 220 to 300-Mev  $\pi^+$  mesons. These data are given in Table II, which contains the distributions of the sum of absorption and charge-exchange processes (row 1) and of each of them separately (rows 2 and 3). The meaning of the fourth row will be given below.

### a. Charge-Exchange Scattering

The charge-exchange scattering of  $\pi^+$  mesons on free nucleons takes place in the  $\pi^+n \rightarrow \pi^0p$  reaction. The character of this process on a nucleus can be determined by comparing the stars accompanying charge-exchange events with those produced in interactions between protons of corresponding energy and the nuclei. The conditions for the production of stars as the result of development of nucleonic cascades may be similar in both cases, since the interaction mean free path of  $\pi^+$  mesons in the energy range under consideration is small compared with the size of the nucleus and the interaction mean free path of protons in it.

Data on the stars produced by protons were obtained in the course of a special proton-beam experiment using the same chamber filling as in the experiments with  $\pi^+$ -meson beams. 280-Mev protons were chosen to ensure their stopping at

TABLE II. Relative multiplicity distribution of stars associated with charge-exchange and absorption of 220 to 300-Mev  $\pi^+$  mesons

Type of event	Multiplicity (number of prongs)					
	0	1	2	3	4	5
Absorption and charge-exchange stars	$5.6 \pm 0.8$	$24.2 \pm 1.8$	$39.4 \pm 2.4$	$22.2 \pm 1.8$	$7.6 \pm 1.0$	$\sim 1$
Charge-exchange stars	$18.5 \pm 3.9$	$52.0 \pm 6.2$	$28.0 \pm 4.6$	$1.5 \pm 1.2$	—	—
Absorption stars F(n)	$2.6 \pm 0.7$	$17.8 \pm 3.0$	$42.3 \pm 2.8$	$27 \pm 2.2$	$9.3 \pm 1.3$	—
Distribution f(n + 1)	$< 1$	$10.8 \pm 1.5$	$51.1 \pm 3.2$	$33.7 \pm 2.6$	$4.4 \pm 0.9$	—

TABLE III. Relative multiplicity distribution f(n) of stars associated with inelastic scattering of 115 to 220-Mev protons

Proton energy Mev	Multiplicity (number of prongs)			
	0	1	2	3
$143 \pm 27$	$11.3 \pm 2.0$	$54.8 \pm 4.4$	$30.5 \pm 3.2$	$3.4 \pm 1.1$
$195 \pm 25$	$10.3 \pm 2.0$	$47.7 \pm 4.3$	$36.6 \pm 3.7$	$5.3 \pm 1.4$
$115 - 220$	$10.8 \pm 1.5$	$51.1 \pm 3.2$	$33.7 \pm 2.6$	$4.4 \pm 0.9$

the end of the chamber. The multiplicity distribution of stars of various energies is given in Table III. It follows from the table that the distribution is independent of the energy over the measured range. We can conclude from the data obtained at lower proton energies that the multiplicity distribution is slightly different from that of Table III. The maximum, nevertheless, remains in the vicinity of one-prong stars.

Comparing the multiplicity distribution of stars associated with the exchange scattering of  $\pi^+$  mesons (Table II, row 2) with that of proton-produced stars (Table III) one can notice a close similarity between the two. This fact shows that the charge-exchange scattering from nuclei is due to a single collision between the incident  $\pi^+$  meson and a neutron of the nucleus.

The angular distribution of photons in the charge-exchange scattering of  $264 \pm 15$  Mev and  $245 \pm 15$  Mev  $\pi^+$  mesons was estimated from the forward/backward ratio in 67 events. This was found to be equal to  $1.76 \pm 0.30$ , which indicates clearly anisotropy of the exchange scattering and of the  $\pi^+$ -meson scattering from free protons in the energy range investigated.

Difficulties connected with the identification of  $\pi^-$  mesons in the chamber did not permit us to estimate with reasonable accuracy the efficiency of the charge-exchange process ( $\pi^+ \rightarrow \pi^-$ ). The cross-section for this process, judging from the two cases observed, is of the order of  $10^{-27}$  cm<sup>2</sup> per fluorine nucleus.

#### b. Production of Stars

The absorption of  $\pi^+$  mesons by nuclei was studied earlier in greater detail at energies below 100 Mev by means of emulsions and cloud chambers.<sup>4-7</sup> An analysis of the stars produced as the result of the absorption of < 100 Mev  $\pi^+$  mesons showed that, in not less than 60% of cases,  $\pi^+$  mesons are absorbed by proton-neutron pairs according to the scheme  $\pi^+ + (pn) \rightarrow pp$ .

The contribution of this process to the absorption of  $\pi^+$  mesons in the energy range investigated in the present experiment can be assessed from a study of the multiplicity distribution of stars. The data for 220 to 300-Mev  $\pi^+$  mesons were analyzed in detail. It can be seen from Table II that two- and three-pronged stars are observed most often in absorption events. This fact can be explained assuming that, as in the low-energy range, the absorption follows the scheme  $\pi^+ + (pn) \rightarrow pp$ , and using the data on

the interaction of protons with nuclei. In fact, since the angle between the protons emitted in the reaction is large (150 to 180°), one only of the fast protons interacts, on the average, in the nucleus. The energy of these protons is close to that used in the auxiliary experiment employing a proton beam. One can expect therefore that the multiplicity distribution of stars produced in the absorption of  $\pi^+$  mesons is  $F(n) = f(n+1)$ , where  $f(n)$  is the proton distribution.

It follows from Table II that the distributions  $F(n)$  and  $f(n+1)$  are very similar (rows 3 and 4). This strengthens the assumption that the reaction  $\pi^+ + (pn) \rightarrow pp$  plays a predominant role in the absorption of 230 to 300-Mev  $\pi^+$  mesons by nuclei. An additional analysis of the multiplicity distribution of stars as a function of  $\pi^+$ -meson energy in the 80 to 300 Mev range showed that the distribution is almost independent of energy. It follows therefore that the absorption of  $\pi^+$  mesons by (p-n) pairs is the main absorption process over the whole range.

It was found by a comparison of the number of events corresponding to the reaction  $\pi^+ + (pn) \rightarrow pp$  with the total number of stars and with the known degree of transparency of nuclei for protons that, for 200-Mev  $\pi^+$  mesons, the absorption by (p-n) pairs in the first interaction occurs in 60 to 70% of cases.

#### c. Production of Charged $\pi$ Mesons by $\pi^+$ Mesons

Six events in which charged  $\pi$  mesons were produced by  $\pi^+$  mesons were observed in the 210 to 300 Mev range. The cross section calculated from these is  $(0.7 \pm 0.3) \times 10^{-27}$  cm<sup>2</sup> per fluorine nucleus. This value is close to that obtained in experiments using a helium-filled diffusion chamber<sup>8</sup> and is also in agreement with the results of experiments using hydrogen.<sup>9</sup>

It is interesting to note that in one only of the six cases an accompanying proton is emitted. Its energy was found to be 40 Mev. This fact indicates that, in the production process, the incident meson collides more often with a virtual meson than with a nucleon.

In conclusion, the authors would like to thank A. A. Tiapkin for a discussion of the results, V. P. Dzheleпов for enabling us to carry out the experiments, and to V. P. Rumiantseva and K. A. Zaitsev for help in the reduction of data.

<sup>1</sup>Mukhin, Ozerov, and Pontecorvo, J. Exptl. Theoret. Phys. (U.S.S.R.) 31, 371 (1956), Soviet Phys. JETP 4, 237 (1957).

<sup>2</sup> Blinov, Lomanov, Meshkovskii, Shalamov, and Shebanov, Приборы и техника эксперимента (Instruments and Meas. Eng.) **1**, 35 (1958).

<sup>3</sup> Blinov, Krestnikov, and Lomanov, J. Exptl. Theoret. Phys. (U.S.S.R.) **31**, 762 (1956), Soviet Phys. JETP **4**, 661 (1957).

<sup>4</sup> Byfield, Kessler, and Lederman, Phys. Rev. **86**, 17 (1952).

<sup>5</sup> J. Tracy, Phys. Rev. **91**, 960 (1953).

<sup>6</sup> G. Bernardini and F. Levy, Phys. Rev. **84**, 610 (1951).

<sup>7</sup> F. H. Tenney and J. Tinlot, Phys. Rev. **92**, 974 (1953).

<sup>8</sup> Kozodaev, Suliaev, Filippov, and Shcherbakov, J. Exptl. Theoret. Phys. (U.S.S.R.) **31**, 701 (1956), Soviet Phys. JETP **4**, 580 (1957).

<sup>9</sup> V. B. Zinov and S. M. Korenchenko, J. Exptl. Theoret. Phys. (U.S.S.R.) **34**, 301 (1958), Soviet Phys. JETP **7**, 210 (1958).

<sup>10</sup> J. O. Kessler and L. M. Lederman, Phys. Rev. **94**, 689 (1954).

Translated by H. Kasha  
187